TD-02-013
04/02

REVIEW OF SSC AND LHC BEAM SCREEN VACUUM EXPERIMENTS

P. Bauer
Fermilab, Technical Division

As part of Fermilab's recent Very Large Hadron Collider (VLHC) feasibility study, a water-cooled photon stop was proposed as a possibility to intercept the intense synchrotron radiation in the high field stage VLHC with minimal plug-power. The photon stop, if feasible, promises not only significant savings in cooling power compared to a solution in which the synchrotron radiation is extracted from a beam screen at cryogenic temperatures, but also virtually removes the synchrotron radiation limitation to beam energy and luminosity in a future VLHC.
A first series of tests is being prepared at the Argonne Advanced Photon Source (APS) synchrotron light source. These tests should verify thermal models and yield information about photo-induced gas and electron desorption as well as X-ray fluorescence from the photon stop exposed to synchrotron radiation. The following presents the results of a literature study on photo-desorption experiments conducted in the context of the Large Hadron Collider (LHC) and the ill-fated Superconducting Super Collider (SSC) vacuum R&D. The photo-desorption coefficients measured in the these tests are an important input parameter to the model that is used to simulate the first photon-stop vacuum test. The photon stop vacuum model is an important tool for the design of the vacuum measurement.

1) Introduction

A detailed summary of the SSC beam screen vacuum experiments was presented by W. Turner [1]. Recently in the context of the LHC beam screen measurements were performed at BINP. They are summarized in [2]. Both, the SSC and LHC efforts consisted in exposing a short length (~1-5 m) of beam-tube to a white synchrotron radiation beam hitting at grazing incidence (~10 mrad). The pressure development with and without radiation was measured to determine the desorption coefficients for the most common UHV gases (H_2, CO, CO_2, H_2O, CH_4). Here, a short review of the photo-desorption experiment results at room temperature, which are of interest in the context of the photon stop test, will be given. Following the procedure initiated by Turner the photo-desorption data will be presented in terms of the following fit

$$h = h_0 \left(\frac{\Gamma}{\Gamma_0} \right)^{-n} \quad \left(\frac{molecules}{photon} \right), \tag{1}$$

where η_0 (molecules/photon) is the desorption coefficient at the reference photon flux Γ_0 (photons/m), Γ (photons/m) is the integrated linear photon flux and ν the slope parameter. Regarding (1) it has to be pointed out, that it is generally assumed that there are two photo-desorption coefficients, η' and η. The former coefficient applies to the desorption of loosely bound ("physisorbed") gases that are for example cryo-pumped to the surface ("secondary desorption"). It is several orders of magnitude larger than η, which describes the desorption of tightly bound ("chemisorbed") surface gases ("primary desorption"). In room temperature experiments, or experiments in which some form of pumping (e.g. pumping through liner-perforations to a low temperature cryo-pumping surface shielded from photon bombardment) is provided, it is η that is being measured, because the desorbed gas is continuously being removed and not allowed to re-adsorb on the surfaces. In room temperature experiments strong thermally induced desorption prevents sticking of the photo-desorbed gas molecules to the walls.

2) SSC Beam-Screen Tests at BNL, UW and BINP

In the context of the SSC beam tube development multiple experiments were conducted, first (before SSC approval under the CDG) at BNL/NSLS and UW/SRC, and later again at BNL/NSLS and finally at BINP/VEPP-2M. At the same time room temperature photo-desorption tests were conducted by the BNL group at the BNL/NSLS [3].
The first cryogenic CDG/BNL/NSLS tests, conducted in a closed geometry (simple steel tube with electrodeposited Cu plating), were limited to a maximum integrated photon flux of 10^{21} photons/m (~1 day of SSC operation) yielding large uncertainty regarding the extrapolation toward larger flux [5]. Subsequently a series of cryogenic measurements was performed in "open geometry" with small samples cut from beam tubes at the SRC in Wisconsin [6]. To obtain data for flux beyond 10^{21} photons/m, a collaboration between the SSC-Lab and BINP/VEPP-2M was launched [7], [8] and a new series of room temperature measurements was conducted at BNL (SSC/BNL/NSLS) [4]. The BINP facility was then used by the CERN team for the LHC related R&D (see chapter 3).

The objective of all these measurements was to find a beam tube material and surface treatment with low photo-desorption coefficients and to determine if a perforated liner system or a simple beam tube was to be preferred. The double tube solution consisting of a perforated liner at a higher temperature, surrounded by a low temperature cryo-pumping tube, was finally adopted. The experimental evidence from BNL tests using copper, aluminum and steel tubes with different surface preparations, indicate that exposure to atmosphere and cleaning solutions render the photo-desorption characteristics to be fairly similar and independent of production. An interesting variant of the Brookhaven experiments (later confirmed at BINP) consisted of rotating the beam tube by 140 degrees followed by a repeated measurement of the desorption coefficient. Comparison with the former photo-desorption results indicated that this previously un-exposed surface had received approximately 25 % of the integrated flux of the previous test, hinting at a considerable amount of reflection from the primarily exposed surface [4]. A summary of the room temperature photo-desorption coefficients for Cu or Cu-plated beam-tube samples measured in the above mentioned experiments is given in Figure 8. The experimental results were parametrized in terms of the initial coefficient η_0, reference photon flux Γ_0 and the exponent ν of fit (1). The parameters are listed in Table 1. The results of the CDG/UW/SRC are not listed in the table. Because of the different nature of the experimental set-up - data in this experiment were obtained in terms of photon-flux per unit surface – the data cannot be compared directly to the other results. The CDG/UW/SRC results are plotted separately in Figure 3.

Table 1: The parameters (initial desorption coefficient η_0 in molecules/photon, reference photon flux Γ_0 is 10^{19} photons/m/sec and the fit-parameter ν of fit (1) for the SSC room-temperature photo desorption experiments on Cu or Cu-plated beam-tube samples.

Gas	**H_2**	**CO_2**	**CO**	**H_2O**	**CH_4**
	CDG/BNL/NSLS - E_c=478 eV, 9 mrad incid., data extrapol. > 10^{21}ph/m, [6];				
h_0	0.058	0.0081	0.012	-	0.00085
n	0.5	0.43	0.45	-	0.47
	BNL /NSLS - E_c=500 eV, 10 mrad incid., [3];				
h_0	0.02	0.0007	0.002	-	0.00013
n	0.5	0.5	0.5	-	0.5
	SSC/BNL/NSLS - E_c=478 eV, 9 mrad incid., data extrapol. > 10^{21}ph/m, largest data set from a large series [9], [4];				
h_0	0.017	0.0025	0.009	-	-
n	0.3	0.4	0.44	-	-
	SSC/BINP/VEPP-2M/1 - E_c=284 eV, 10 mrad incid., data extrapol. > 10^{22}ph/m, [19];				
h_0	0.034	0.0012	0.0057	-	0.0007
n	0.4	0.45	0.45	-	0.45
	SSC/BINP-VEPP-2M/2 - E_c=284 eV, 10 mrad incid., data extrapol.> 10^{22}ph/m, [17];				
h_0	0.05	-	0.01	-	-
n	0.55	-	0.55	-	-

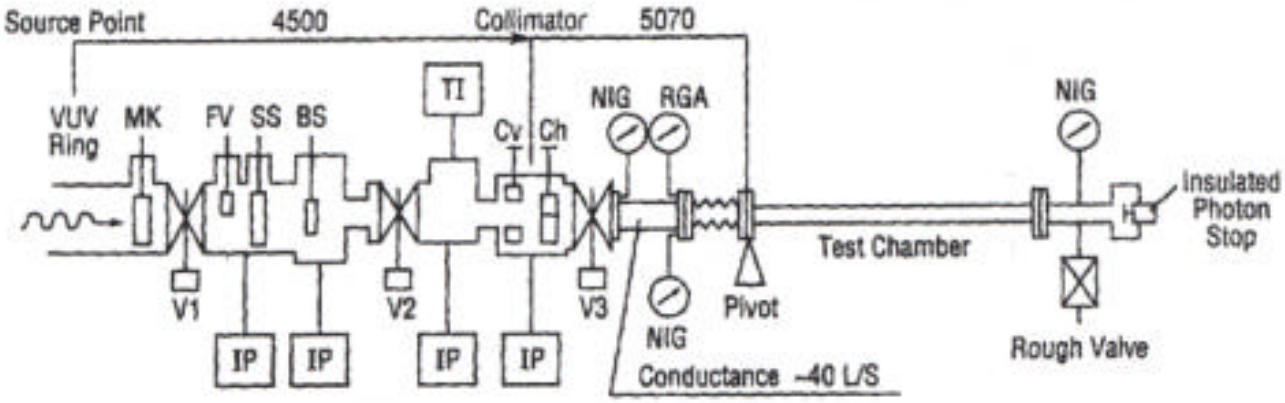

Figure 1: Schematic diagram of NSLS beam-line U10b, including test-chamber. Components: Mk-mask for front and end valve V1; FV – fast valve; SS – safety shutter; BS – beam stop, MB – mirror box; V2 – isolation valve; CB – collimator box with adjustable vertical – CV and horizontal – CH – collimators; V3 – isolation valve; B – bellows; O1 and O2 – orifices;

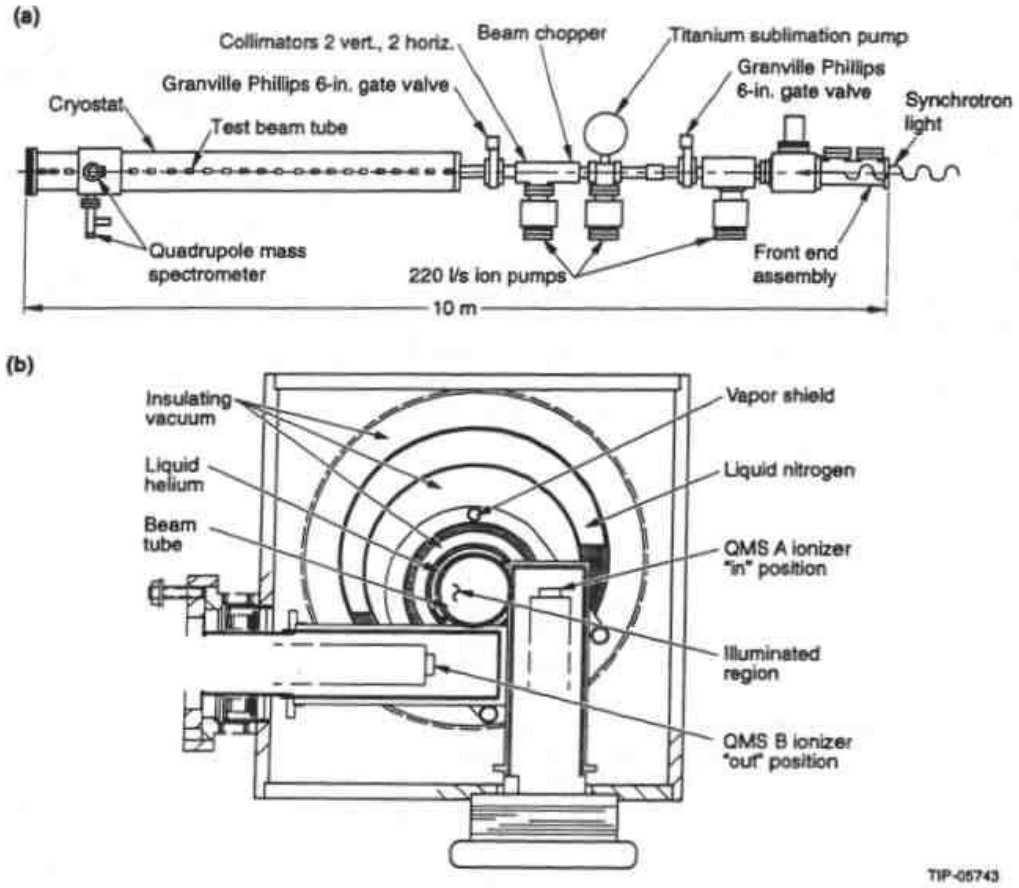

Figure 2: CDG cold tube photo-desorption apparatus at BNL/NSLS, a) cryostat, b) detectors.

The measurement set-up of the CDG-BNL/NSLS measurement is given in Figure 2, the room temperature set-up at BNL/NSLS is shown in Figure 1 and the BINP/VEPP-2M measurement set-up (similar for both the SSC and LHC experiments) is given in Figure 6.

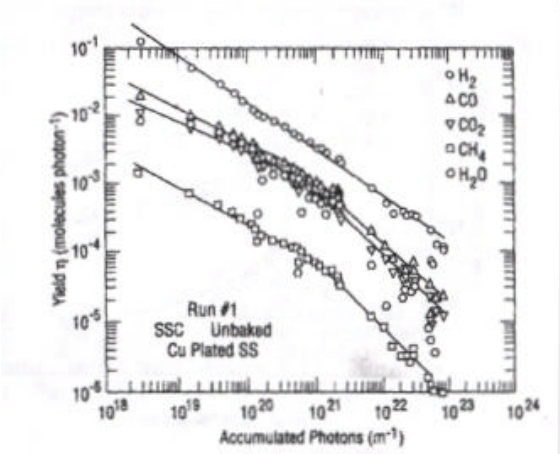

FIG. 2. Molecular desorption yields for unbaked copper plated nitronic 4
(run #1).

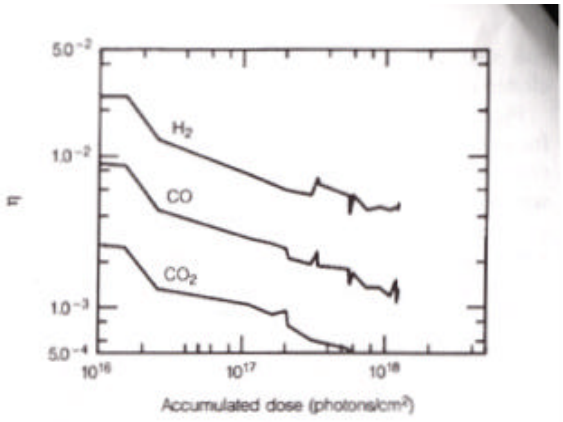

FIG. 7. η vs accumulated photon dose for a room-temperature copper-plated beam tube. Data are from Ref. 2.

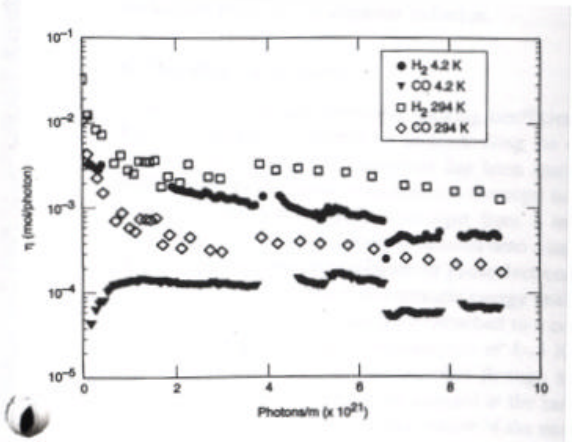

FIG. 4. $\eta(H_2)$ and $\eta(CO)$ vs integrated photon flux for electrodeposited Cu. Data are shown for 4.2 and 294 K experiments.

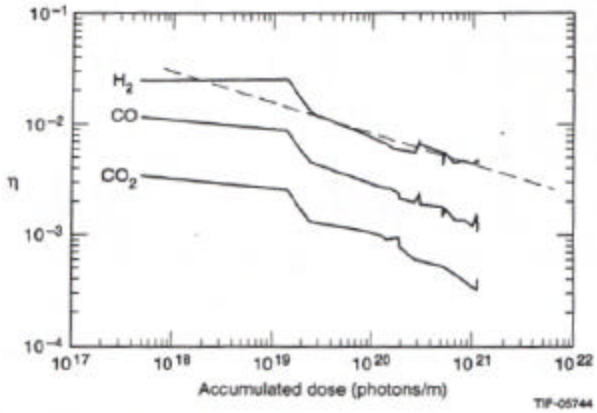

Figure 5. Room-temperature photodesorption data from the CDG experiment.[16]

Figure 3: Results of photo-desorption measurements; Upper left: BNL/NSLS room temperature tests; Upper right: CDG room temperature measurement at UW/SRC; Bottom left: SSC-BINP tests at VEPP-2M in room temperature and cryogenic conditions; Bottom right: CDG-BNL/NSLS room temperature desorption;

3) LHC Beam-Screen Tests

Many different experiments were conducted by CERN in the context of the LEP and LHC machine R&D. The following will briefly review the most important experiments done in the context of the LHC machine studies. These include tests at the DCI ring at Orsay, the EPA electron-positron accumulator at CERN and most recently the VEPP-2M ring at BINP. The experiment at the DCI positron storage ring at Orsay used 3.75 keV E_c

radiation at a grazing incidence (11 mrad) on an OFHC Cu tube at room-temperature [10], [11]. The tube went through a sophisticated cleaning procedure: alkaline etch, vapor degreasing in perchlorethylene at 121°C, alkaline deoxidization, acid etch (pickling in HCl), passivation in chromic acid/H_2SO_4 bath, rinsing in demineralized water, drying with N_2 gas, vacuum braze, alkaline deoxidization, 150°C in-situ bake-out for 24 hrs;
The dose dependent desorption coefficients found and fitted with the Turner model are given in Table 3. The Turner model fits only within a factor 2 for H_2, the agreement is better for other gases, H_2O data are badly fitted and experimental results "unusual";
The activation energies of the different gas species for thermal desorption were derived from the (exponential E_{act}/kT) temperature dependence of the pressure-drop after interruption of the irradiation and the subsequent cool-down of the irradiated tube from 70°C to ambient. The desorption-yield remains constant for all gases except for H_2O and O_2 (factor 5 increase). A substantial difference in activation energy before and after irradiation was found (see Table 2), indicating an increase of "loosely" bound surface states with photon bombardment. The DCI experiment setup is shown in Figure 5.

Table 2: Activation energies (eV/molecule) of common UHV gases before and after irradiation.

gas	H_2	CO_2	CO	H_2O	CH_4
before	0.15	0.27	0.13	0.42	0.12
after	0.5	1.41	1.66	0.55	0.67

A similar setup was used in the vacuum tests at the EPA, which served primarily the purpose of measuring adsorption isotherms at low temperature. The characteristic radiation energy was 45.3 eV. The experiments were conducted at normal incidence and at various temperatures [12]. The room temperature desorption results are listed in Table 3. The EPA beam-line set-up was later used for the COLDEX experiment [13], a mock-up of the LHC vacuum system.
The most important cryogenic vacuum experiments were conducted at BINP [14]. The experimental setup is shown in Figure 6. The most important part of the diagnostics is shown in the left upper insert – it consists of a high temperature (77 K – 300 K) chimney leading the desorbed molecules to the RGA with minimal sticking to the chimney walls. The measurement consisted in finding the pressure rise due to photo-induced desorption by subtracting the background (pressure without synchrotron radiation, typically $4 \cdot 10^{-10}$ Torr) from the pressures measured by the RGA and relating it to the desorption coefficient via the photon flux and the calculated pumping speed of the cryo-pump within the beam screen assembly. Table 3 summarizes the desorption coefficients measured on Cu-plated beam tubes in the experiments discussed above. Figure 4 shows plots of the desorption measurement results.

Table 3: The parameters (initial desorption coefficient η_0 in molecules/photon, reference photon flux Γ_0 is 10^{19} photons/m and the fit-parameter ν of fit (1) for the CERN photo-desorption experiments on Cu-plated beam-tubes.

Gas	**H_2**	**CO_2**	**CO**	**H_2O**	**CH_4**
	DCI - E_c=3.75 keV, grazing incidence (11 mrad), [10], [11];				
h_0	0.0013	0.0009	0.0006	0.001	0.00013
n	0.2	0.23	0.29	0.6	0.29
	EPA - E_c=45.3 eV, normal incidence, [12];				
h_0	0.0015	0.0012	0.00065	0.00065	0.00015
n	0.26	0.35	0.35	0.35	0.3
	BINP - E_c=50 eV, grazing incidence (77 K). [14]				
h_0	0.0013	0.00003	0.00015	-	0.00002
n	0.28	0.4	0.28	-	0.25

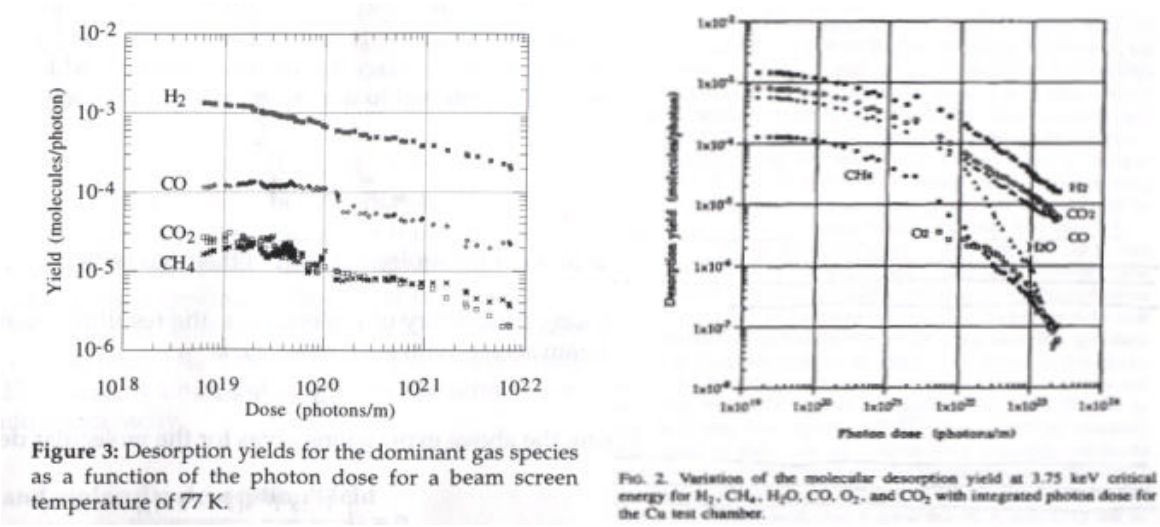

Figure 3: Desorption yields for the dominant gas species as a function of the photon dose for a beam screen temperature of 77 K.

FIG. 2. Variation of the molecular desorption yield at 3.75 keV critical energy for H_2, CH_4, H_2O, CO, O_2, and CO_2 with integrated photon dose for the Cu test chamber.

Figure 4: Desorption yield at 77 K – BINP (left) and at 300 K - DCI measurement (right).

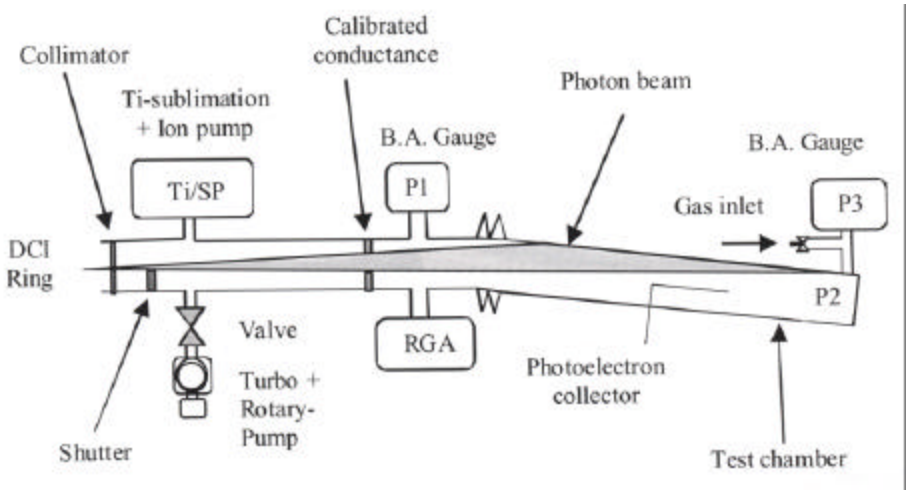

Figure 5: Beam-line setup used in both the CERN/EPA and Orsay/DCI experiments.

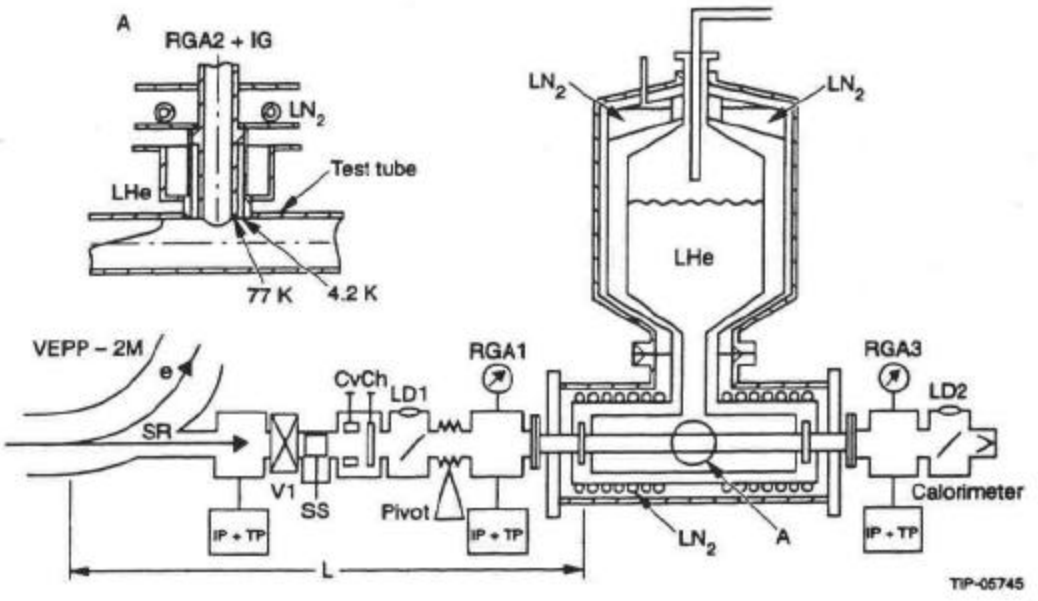

Figure 6: Setup for beam screen vacuum measurement with LHC beam screen at BNP.

4) Electron Desorption Experiments

CERN conducted several experiments to estimate the photo-induced electron yield. We will briefly report here on the experiment at the DCI positron storage ring at Orsay using 3.75 keV E_c radiation [11] and the experiments at the EPA ring at CERN with 194 eV E_c radiation [15].

The electron yield in both experiments were measured with an electrode, made from a 1mm diameter steel wire held at a 1 kV potential. The collected current (~μA) is proportional to the number of electrons extracted from the surface by the impinging flux of radiation. Both experiments found the largest yields for non baked surfaces, especially in the case of Al. Figure 7 shows the results from the DCI experiments on a Cu-surface. The best EPA data on Cu are almost an order of magnitude smaller. In general the

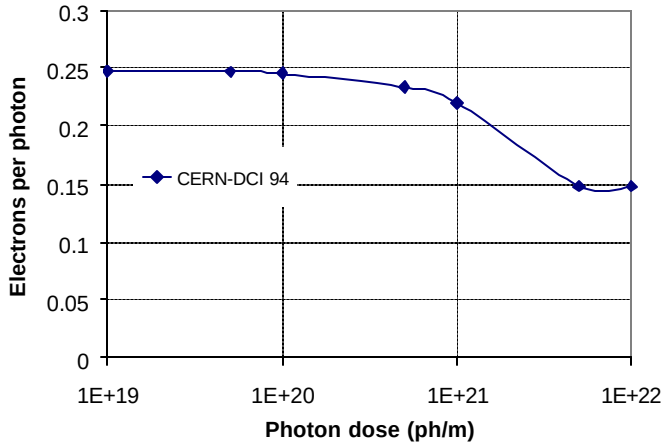

Figure 7: Photo-electron yield measured in 3.75 keV E_c synchrotron radiation at the DCI ring.

desorption yields decrease as a function of integrated dose and are generally reduced for cleaner surfaces. The above noted DCI experimental result can be parametrized with (2) in terms of the integrated linear flux Γ (photons/m).

$$h_e(\Gamma) = 2\cdot 10^{-45}\,\Gamma^2 - 3\cdot 10^{-23}\,\Gamma + 0.25 \qquad \left(\frac{electrons}{photon}\right) \tag{2}$$

5) Summary of Desorption Measurements for SSC and LHC

The desorption data in Table 1 and Table 3 reveal a considerable spread. They were measured mostly on samples, that were submitted to cleaning procedures similar to those in the accelerator setting. Figure 8 shows a summary of the H_2 data. This spread is partly due to differences in incidence angle (the smaller the angle the larger the desorption), differences in the radiation energy spectrum and differences in temperature, but mostly explained by variations in the surface conditions and the general roughness of the RGA and BA data. The data in Figure 8 clearly separate into two groups: a band of results obtained in the context of the SSC R&D and by almost one order of magnitude smaller data produced by CERN in the context of the LHC. The general tendency of lower desorption yields found by the CERN group is as well reflected in the desorption plot shown in [16]. The exact cause of this discrepancy is not known. The two lowest sets of data, however, the CERN/DCI and LHC/BINP data, are exceptional insofar as the sample tube underwent intensive cleaning in the CERN/DCI case and the results of the LHC/BINP experiments were obtained at 77 K (no room temperature data could be found). For these reasons the CERN/DCI and LHC/BINP results may therefore not be

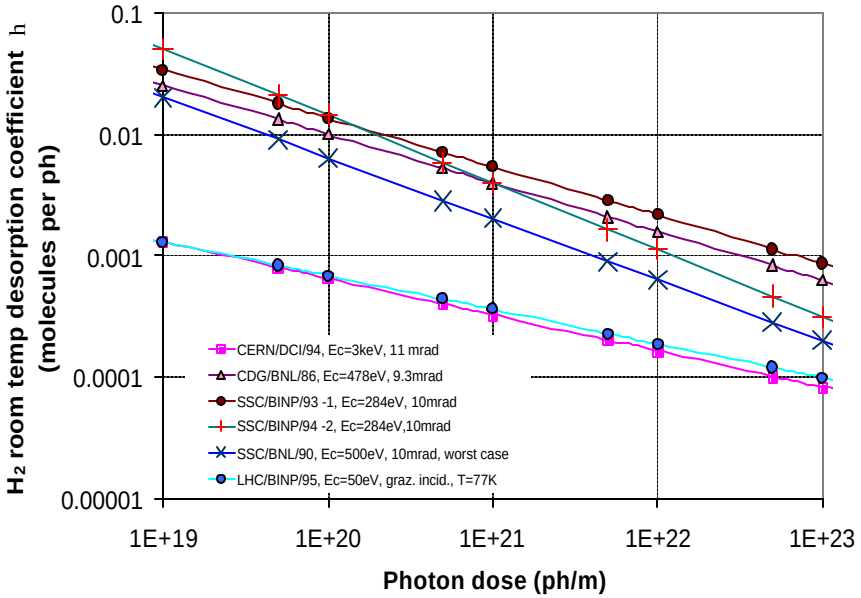

Figure 8: Summary of measured desorption coefficients for H_2 from Cu or Cu-plated beam-tubes, mostly at room temperature. Curves shown represent experimental data approximated with fit (1).

Table 4: Average of room temperature desorption parameters from Table 1 and Table 3 (excluding CERN/DCI, CERN/EPA and LHC/BINP) according to (1). The reference flux Γ_0 in all cases is 10^{19} ph/m.

gas j	η_{0j} (molec/phot) –Copper surface	ν_j
H_2	0.036	0.45
CH_4	0.0006	0.48
CO	0.0077	0.48
CO_2	0.0031	0.45

applicable to the photon stop case, which will operate above room temperature and will undergo minimal cleaning only (degreasing and in-situ bake-out at moderate temperature). Furthermore, the CERN/EPA data were taken with normal incidence of the radiation beam and therefore not included either. Table 4 lists the average desorption parameters for the most common gases, calculated from the data in Table 1 and Table 3. The CERN/DCI, CERN/EPA and LHC/BINP data were not included in the average.

6) Applying SSC and LHC Photo Desorption Data to the Photon Stop Test

Three issues arise when applying the above data to the case of the photon stop test. First, the synchrotron radiation in the VLHC will be harder than in the LHC or SSC. The latest VLHC design is characterized by a 8 keV critical energy of the synchrotron radiation spectrum. Second, the radiation will strike the photon stop at approximately normal incidence, instead of the grazing incidence, which is relevant in beam-screen arrangements. The desorption yield is expected to drop at larger incidence angles. Third, with the radiation striking at normal incidence, the desorption data have to be renormalized to an incident flux per surface area rather than per m of beam tube.
Figure 9 (from a presentation by O. Groebner at the 2000 VLHC workshop) shows the evolution of the desorption coefficients toward larger critical energies, such as those in

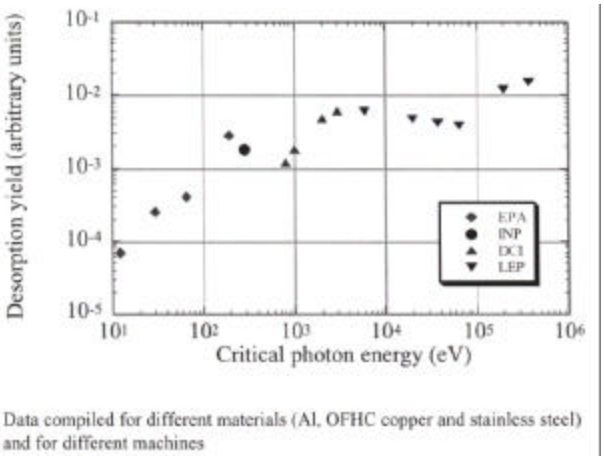

Figure 9: Desorption yield for H_2 at different critical energies of the synchrotron radiation spectrum [courtesy of O. Groebner, VLHC workshop Sept. 2000].

the VLHC. Reference [16] contains a similar plot. These plots indicate a saturation of the desorption yields at higher photon energies. Therefore we believe that, in a rough

approximation, the desorption data measured in the context of the SSC and LHC for a range of critical energies between 50 eV and 3.7 keV are similar (within a factor 2) to those at 8 keV. The existing experimental evidence of the expected decrease of desorption yield at normal incidence compared to grazing incidence is meager. The CERN/EPA data listed in Table 3 can be used to give a quantitative estimate of this trend. Figure 10 shows a comparison of the H_2 data generated in the CERN/EPA experiment versus the average H_2 desorption yield of Table 4. This comparison suggests that the effect is substantial, of one order of magnitude.

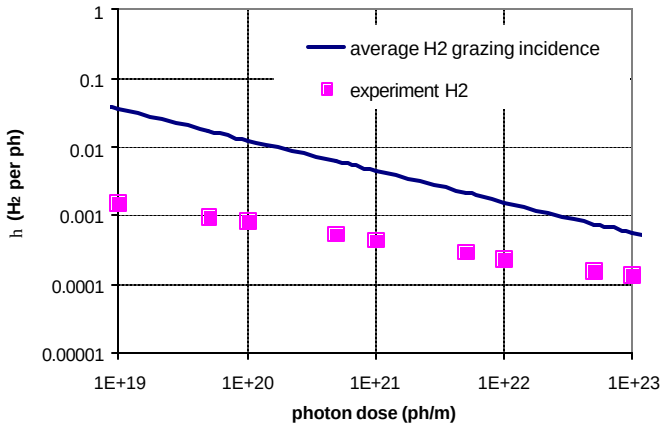

Figure 10: Comparison of CERN/EPA desorption yield measurements for H_2 at normal incidence vs. the average grazing incidence data from Table 4. Measurements on Cu-samples at room temperature [12].

The desorption data discussed throughout this chapter have to be renormalized to surfaces in order to be applicable to the photon stop case. The CDG/UW/SRC data have been obtained for a radiation flux normalized on the (flat) sample surface. A straightforward renormalization of the average desorption yields from Table 4 fits the CDG/UW/SRC data well (Figure 11). The renormalization consists in dividing the linear radiation flux (photons/m) by the unit beam-tube surface area per m of beam tube exposed to the incoming radiation Δ m^2/m, where Δ is approximately the circumference of the beam tube in the experiments. This finding is corroborated by the observation of multiple reflection and scattering from the primary incidence area. The Δ chosen in the comparison of Figure 11 is πd, where d=80 mm, which is representative of the beam tube diameter in the above listed experiments (32 mm – 131 mm tube diameters).
Therefore, in the following, the phenomenological desorption law (1) will be applied to surface flux by renormalizing Γ_0'=Γ_0/Δ (Δ=0.25 m).

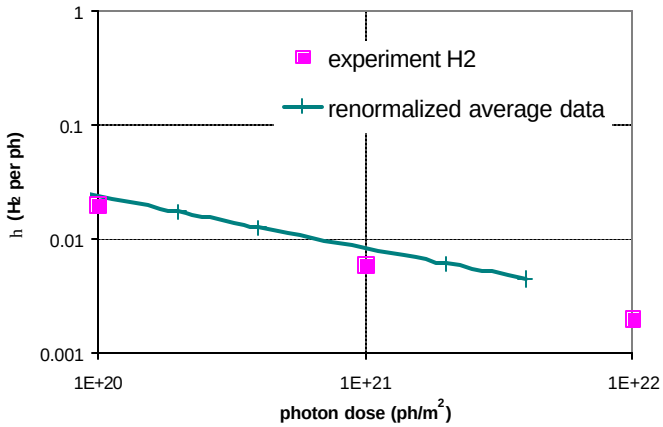

Figure 11: Comparison of CDG/UW/SRC H_2 desorption data with "renormalized" average H_2 desorption data from Table 4. The beam tube diameter in the renormalization was assumed to be 0.25 m.

References:

[1] W.C. Turner, "*Beam Tube Vacuum in Future Superconducting Proton Colliders*", SSCL Preprint-564, Oct. 1994

[2] O. Groebner, "*The VLHC Vacuum System*", Proceedings of the 1997 Particle Accelerator Conference, Vancouver, Sept. 1997

[3] C.L. Foerster, H. Halama, C. Lanni, *"Photon-Stimulated Desorption Yields from Stainless Steel and Copper-Plated Beam Tubes with Various Pretreatments*", J. Vac. Sci. Techn. A8/2856, 1990

[4] C.L. Foerster, C. Lanni, I. Maslennikov, W. Turner, "*Photon Desorption Measurements of Copper and Copper Plated Beam Tubes for the SSCL 20 TeV Proton Collider*", J. Vac. Sc. Technol. A12(4), 1673, 1994

[5] D. Bintinger, P. Limon, H. Jostlein, D. Trbjovic, "*Status of SSC Photo-Desorption Experiment*", SSC-102, 1986

[6] D. Bintinger, P. Limon, R. Rosenberg, *"Photodesorption from Copper Plated Stainless Steel at Liquid Helium Temperature and Room Temperature*", J. Vac. Sci. Technol., A7 (1), 59, 1989

[7] V.V. Anashin, O.B. Malyshev, V.N. Osipov, I.L. Maslennikov, W. C. Turner, "*Investigation of Synchrotron Radiation-Induced Photodesorption in Cryosorbing Quasiclosed Geometry*", J. Vac. Sci. Technol. A 12(5), 2917, 1994

[8] V.V. Anashin et al., "*Cold Beam Tube Photodesorption and Related Experiments for the Superconducting Super Collider Laboratory 20 TeV Proton Collider*", J. Vac. Sci. Technol. A 12(4), 1663, 1994

[9] W.C. Turner, "*Vacuum Analysis of the ASST II Liner*", Presentation for the 80 K liner review, SSCL, April 1993

[10] A. Mathewson, O. Groebner, P. Strubin, P. Marin, R. Souchet, "*Comparison of Synchrotron Radiation Induced Gas Desorption from Al, Stainless Steel and Cu Chambers*", AIP Conf. Proc., 236 or CERN/AT-VA/90-21 note, 1990

[11] O. Groebner, A. Mathewson, P. Marin, *"Gas Desorption from an Oxygen Free High Conductivity Copper Vacuum Chamber by Synchrotron Radiation Photons*", J. Vac. Sci. Technol. A12(3), 846, 1994

[12] V. Baglin, Doctoral Thesis, Universite Denis Diderot, Paris 7, Mai 1997

[13] V. Baglin, I.R. Collins, C. Gruenhagel, O. Groebner, B. Jenninger, "*First Results from Coldex Applicable to the LHC Cryogenic Vacuum System*", Proceedings of the 7th European Particle Accelerator Conference, Vienna, Austria, or LHC Project Report 435, 2000

[14] R. Calder, O. Groebner, A.G. Mathewson, V.V. Anashin, A. Dranichnikov, O.B. Malyshev, "*Synchrotron Radiation Induced Gas Desorption from a Prototype LHC Beam Screen at Cryogenic Temperature*", LHC Project Note 7, Sept. 1995

[15] V. Baglin, I.R. Collins, O. Groebner, *"Photo-electron Yield and Photo Reflectivity from Candidate LHC Vacuum Chamber Materials with Implications to the Vacuum Chamber Design"*, Proceedings of the 1998 European Particle Accelerator Conference, Stockholm, 1998, or LHC Project Report 206, 1998
[16] A.G. Mathewson, O. Groebner, *"Thermal Outgassing and Beam Induced Desorption"*, p. 224 in Handbook of Accelerator Physics and Engineering, A. Chao, M. Tigner, editors, World Scientific, 1998